Published in final edited form as:
Mol Imaging. 2013 ; 12(1): 17–27.

Development and Characterization of ^{89}Zr-Labeled Panitumumab for Immuno–Positron Emission Tomographic Imaging of the Epidermal Growth Factor Receptor

Albert J. Chang[*], **Ravindra A. De Silva**[*], and **Suzanne E. Lapi**
Departments of Radiation Oncology and Radiology, Mallinckrodt Institute of Radiology, Washington University School of Medicine, St. Louis, MO.

Abstract

The epidermal growth factor receptor (EGFR) is overexpressed in the majority of malignancies and has been associated with poor outcomes. Panitumumab, an anti-EGFR monoclonal antibody that binds to the extracellular binding domain of EGFR, is increasingly used with radiotherapy and chemotherapy but has associated toxicities. The purpose of this study was to develop and characterize a novel targeted imaging agent for the EGFR using radiolabeled panitumumab. Flow cytometry studies were performed to evaluate EGFR expression in several cell lines. Desferrioxamine-Bz-NCS (DFO) was conjugated to panitumumab and labeled with ^{89}Zr. Cell uptake studies were performed in four cell lines. For biodistribution studies and micro–positron emission tomography/computed tomography (PET/CT), mouse xenograft models were generated using the same cell lines. PET was performed, and tumors and select organs were harvested for biodistribution studies. Panitumumab was radiolabeled with ^{89}Zr with high radiochemical purity and specific activity and was found to be stable in serum. Cell binding studies demonstrated that radiotracer uptake in cells correlated with the degree of EGFR expression. MicroPET/CT imaging studies demonstrated a high intensity of ^{89}Zr-panitumumab in A431 and HCT 116 tumors in comparison with the EGFR-negative tumors. Biodistribution studies confirmed the results from the imaging studies. ^{89}Zr-panitumumab imaging of EGFR-positive tumors demonstrated levels of radiotracer uptake associated with EGFR expression.

Targeted therapy is increasingly used for cancer therapy. The epidermal growth factor receptor (EGFR), which is overexpressed in many malignancies and associated with poor outcomes, is a known therapeutic target.[1] EGFR is a member of the ErbB tyrosine kinase receptor family and is composed of an extracellular ligand binding domain, a hydrophobic transmembrane domain, and an intracellular tyrosine kinase domain. Binding of its natural ligands, epidermal growth factor or transforming growth factor a, to the extracellular domain activates downstream signaling to promote cell proliferation, angiogenesis, tumor invasion,

Address reprint requests to: Suzanne E. Lapi, PhD, Department of Radiology, Mallinckrodt Institute of Radiology, Washington University School of Medicine, Campus Box 8225, St. Louis, MO 63110; lapis@mir.wustl.edu.
[*]Authors who contributed equally to this work.

Financial disclosure of authors and reviewers: None reported.

metastasis, and cell survival.[2,3] Both monoclonal antibodies and small molecule inhibitors have been used to block the downstream signaling mechanisms of EGFR.[4]

Panitumumab (Vectibix, Amgen, Thousand Oaks, CA) is a fully humanized IgG2 antibody that binds with high affinity to the extracellular ligand binding domain of EGFR. Panitumumab is approved by the Food and Drug Administration for the treatment of refractory, metastatic colorectal cancer.[5] Many clinical trials are also actively testing the efficacy of panitumumab for treatment of other malignancies, including non–small cell lung cancer, esophageal cancer, and pancreatic cancer.[6] Although panitumumab is widely used in the clinic, little is known about its pharmacokinetics and the optimal dosing regimen for treatment response.[7] Furthermore, EGFR status of the primary tumor may not correspond to EGFR expression in metastatic tumor tissue.[8,9]

Immuno–positron emission tomography (PET) may be used to characterize the molecular phenotype of tumors. This strategy involves the conjugation of positron-emitting radionuclides to antibodies[10] such as panitumumab. ImmunoPET may be used to verify the EGFR expression level obtained from a biopsy specimen, as well as provide a more comprehensive view of tumoral EGFR expression in comparison with that obtained from staining a biopsy specimen alone. In addition, immunoPET may be used to characterize EGFR expression in metastatic lesions, which may be inaccessible for biopsy, too numerous, or too invasive for biopsies to be performed. In the era of personalized medicine, immunoPET is also a method to noninvasively monitor the in vivo pharmacokinetics of panitumumab for individualized patient dosing.[10]

Several studies have evaluated radiolabeled anti-EGFR antibodies for imaging EGFR expression.[11–20] The majority of these studies have been performed with cetuximab, a chimeric IgG1 antibody that also binds to the extracellular domain of EGFR.[9] Although no trials have directly compared panitumumab to cetuximab for clinical efficacy, it has been suggested that in animal models, panitumumab may possess superior tumor targeting over cetuximab.[20]

Panitumumab-based PET probes for imaging EGFR have been reported with the positron-emitting radioisotopes ^{86}Y ($T_{1/2}$ 5 14.74 hours) and ^{64}Cu ($T_{1/2}$ 5 12.7 hours).[18,20,21] These probes are limited by the relatively short half-lives of the radioisotopes when compared to the equilibration time required to achieve optimal tumor to nontumor ratios with antibodies. Alternative radioisotopes, such as iodine 124 (^{124}I; $T_{1/2}$ 5 100.4 hours) and zirconium 89 (^{89}Zr; $T_{1/2}$ 5 79.4 hours), which have compatible half-lives for immunoPET with intact antibodies, may be preferable.[10] A disadvantage of ^{124}I is the rapid degradation of the radioiodinated antibody on cellular internalization followed by iodine clearance from the target cells. As a result, images using internalizing radiolabeled antibodies often lack resolution with low tumor to background ratios and are not representative of actual antibody uptake.[22] In contrast to ^{124}I, ^{89}Zr is trapped intracellularly in lysosomes on antibody internalization, resulting in images with improved contrast that are representative of antibody distribution.[22] Recently, a facile preparation method for ^{89}Zr-radiolabeled antibodies was introduced to facilitate further exploration of ^{89}Zr-immunoPET imaging.[23]

Multiple studies have demonstrated the feasibility of ^{89}Zr-radiolabeled antibodies for preclinical molecular imaging and in clinical trials.[19,24–28]

The aim of this study was to develop and characterize ^{89}Zr-radiolabeled panitumumab for in vivo imaging of EGFR expression. Quantitative PET imaging studies were performed in preclinical models to evaluate the relationship between radiotracer uptake and EGFR expression levels as determined by histology.

Materials and Methods

Flow Cytometry

A431 vulvar epidermoid carcinoma, HCT116 colorectal cancer, MDA-MB435 breast cancer, and T47D breast cancer cells (American Type Culture Collection, Manassas, VA) were grown in Dulbecco's Modified Eagle Medium (Invitrogen, Carlsbad, CA) supplemented with 10% fetal bovine serum until 80% confluent. Cells were harvested with trypsin, washed with phosphate-buffered saline (PBS), and incubated on ice with 20 μg/mL panitumumab. After 1 hour, cells were washed with PBS and incubated with fluorescein isothiocyanate (FITC)-conjugated goat antihuman IgG (Sigma-Aldrich, St. Louis, MO) for 30 minutes. EGFR expression was quantified by calculating the mean fluorescence intensity of fluorescein-positive cells as analyzed with the FACSAria Flow Cytometer (Becton Dickinson, Franklin Lakes, NJ).

^{89}Zr Production and Antibody Labeling

^{89}Zr was produced via the ^{89}Y(p,n)^{89}Zr nuclear reaction using the CS-15 cyclotron (Cyclotron Corporation, Berkeley, CA) and separated via ion exchange as previously described,[29,30] with a resulting specific activity of 8.1 to 15.4 GBq/μmol (220–418 mCi/μmol). Panitumumab was incubated with desferrioxamine (Df-Bz-NCS) (Macrocyclics, Dallas, TX) in 0.1 M $NaHCO_3$ buffer pH 9.0 for 30 minutes. The resulting product, Df-Bz-NCS-panitumumab, was purified via Zeba Spin Desalting Columns (Pierce Biotechnology, Rockford, IL). ^{89}Zr was complexed with Df-Bz-NCS-panitumumab at a ratio of 222MBq/mg (6 mCi/mg) of antibody in 0.5 M HEPES buffer pH 7.0 at 37°C for 1 hour with constant agitation. ^{89}Zr-panitumumab was purified with Zeba Spin Desalting Columns, and radio-chemical purity was determined by radio–instant thin layer chromatography (-ITLC) (silica) using a mobile phase of 50 mM diethylenetriamine pentaacetic acid (DTPA) and analytical size-exclusion chromatography (Superose 12 10/300 GL, GE Healthcare, Piscataway, NJ) with 20 mM HEPES and 150 mM NaCl (pH 7.3) eluted at a flow rate of 0.75 mL/min. *Millenium* 32 software (Waters, Milford, MA) was used to quantify chromatograms by integration. ^{89}Zr-panitumumab was incubated at 37°C with human serum for 1, 2, 3, and 7 days and evaluated for stability with size-exclusion chromatography.

In Vitro Cell Uptake Studies

Cell uptake studies were performed with the prepared ^{89}Zr-panitumumab. A431, HCT116, MDA-MB435, and T47D cells were suspended in microfuge tubes at increasing concentrations ranging from 0.5 to 5 × 10^6 cells in 500 μL PBS. Approximately 37 kBq of ^{89}Zr-Df-Bz-NCS-panitumumab in 50 μL was added to each tube (n 5 3) and agitated on

an orbital mixer for 60 minutes at 25°C. Cells were pelleted by centrifugation, washed twice with PBS, and subsequently counted for ^{89}Zr activity using a Beckman 8000 gamma-well counter (Beckman, Fullerton, CA). The specific binding was calculated as the ratio of bound radioactivity to the total amount of administered activity and was corrected for background. To determine binding specificity, additional studies were performed with the addition of 100 μg of nonradiolabeled panitumumab in the HCT 116 model.

In Vivo Biodistribution Studies

All animal experiments were conducted in compliance with the Guidelines for the Care and Use of Research Animals established by Washington University's Animal Studies Committee. In vivo biodistribution studies were performed with athymic nude mice to determine the uptake of panitumumab in A431, HCT116, MDA-MB435, and T47D xenografts in relation to normal organs. Four × 10^6 cells were injected into the right flank of athymic nude mice 6 to 8 weeks of age. All tumors were placed in the same locations in the animals. After tumors grew to approximately 200 mm^3 (volume 5 length × width × height × π/6), 0.56 MBq/4 μg (15 μCi) of ^{89}Zr-panitumumab was administered via intravenous tail vein injection. Five mice per each tumor type were sacrificed by cervical dislocation at 24 and 120 hours postinjection, and tumor and select organs were harvested. Specific uptake for each tissue was measured with background and decay correction and expressed as percent injected dose per gram of tissue (%ID/g) as calculated by normalization to the total activity injected. A known amount of injected activity was used as a standard for comparison.

MicroPET Studies

MicroPET/CT experiments were performed with the Inveon MicroPET/CT scanner (Siemens, Knoxville, TN). Mice were administered ^{89}Zr-panitumumab (2.96–3.7 MBq/20–25 μg in 100 μL 0.9% sterile saline) via tail vein injection. At 24 and 120 hours postinjection, three mice per each tumor type were anesthetized with 2% isoflurane and imaged by PET and computed tomography (CT). Twenty-minute PET static images were collected and coregistered with CT using image display software (Inveon Research Workplace, Siemens). Regions of interest including the tumor and muscle were contoured, and the standardized uptake values for tumors were determined using the formula: SUV 5 [(MBq/mL) × (animal wt (g))/injected dose (MBq)].

Immunofluorescence

Tumors were harvested after completion of microPET/CT imaging studies and immediately fixed in 10% formalin. After allowing for the radioactivity to decay to background levels, tumors were embedded in paraffin. Five-micron sections were prepared and blocked in Dako Protein Block (Dako, Carpinteria, CA) for 30 minutes at room temperature. Antigen retrieval was performed in a citrate-based buffer using a pressure cooker (Biocare Medical, Concord, CA). The sections were incubated with rabbit polyclonal anti-EGFR primary antibody (1:200; Abcam, Cambridge, MA) overnight at 4°C and visualized with Alexa Fluor 555– conjugated goat antirabbit IgG (1:200; Invitrogen). Sections were mounted with SlowFade Gold antifade reagent with 4,6-diamidino-2-phenylindole (DAPI) (Invitrogen) and coverslipped. Images were obtained with a Soft Imaging Solutions FVII cooled

monochrome digital camera, Peltier cooled to −10°C (Olympus America, Center Valley, PA).

Statistical Analysis

The unpaired, two-tailed Student *t*-test was used for data analysis. Differences at the 95% confidence level ($p < .05$) were considered statistically significant.

Results

Panitumumab Conjugation, Radiolabeling, and Stability Testing

Panitumumab was conjugated to Df-Bz-NCS and radio-labeled with ^{89}Zr The number of Df-Bz-NCS per antibody was approximately 1.6. The radiolabeling efficiency was 82.6% ± 5.8%, the radiochemical purity was 98.2 ± 1.3%, and the specific activity was approximately 133.2 MBq/mg (3.6 mCi/mg) ($n = 6$). ^{89}Zr-panitumumab was demonstrated to be stable up to 7 days in serum at 37°C with no visible degradation products on size-exclusion high-performance liquid chromatography (HPLC) analysis (Figure S1 available in the online version only).

Flow Cytometry and Cell Association Studies

To evaluate the EGFR expression levels in A431 epidermoid, HCT116 colorectal, MDA-MB435 breast, and T47D breast cancer cell lines, flow cytometry was performed with panitumumab and a FITC-conjugated antihuman secondary antibody. A431 cells (99.2% EGFR positive) demonstrated a greater EGFR expression level when compared to HCT-116 cells (42.4% EGFR positive). The T47D (6.3% EGFR positive) and MDA-MB435 (0% EGFR positive) breast cancer cell lines exhibited minimal and no expression of EGFR, respectively (Figure 1).

Cell uptake studies demonstrated a correlation between EGFR expression in vitro and ^{89}Zr-panitumumab uptake (Figure 2). ^{89}Zr-panitumumab uptake was 76.4- and 9.9-fold higher in the A431 cells and HCT116 cells, respectively, when compared to the EGFR-negative T47D and MDA-MB435 cell lines, in which there was minimal to no uptake (see Figure 2B). Specificity of binding was demonstrated with the addition of excess unlabeled panitumumab, which abrogated ^{89}Zr-panitumumab uptake in HCT116 cells to levels similar to those observed in the EGFR-negative cell lines (see Figure 2).

Biodistribution Studies

Biodistribution studies with ^{89}Zr-panitumumab were performed in athymic nude mice bearing A431and HCT116 at 24 and 120 hours postinjection and in nude mice bearing T47D and MDA-MB435 at 120 hours postinjection. A431 tumoral uptake of ^{89}Zr-panitumumab was 17.3 ± 0.3 %ID/g at 24 hours and continued to rise to 32.9 ± 4.5 %ID/g at 120 hours, resulting in tumor to muscle ratios of 5.2 and 16.4, respectively. ^{89}Zr-panitumumab uptake in HCT116 tumors was 10.6 ± 1.0 and 19.8 ± 4.1 %ID/g at 24 and 120 hours ($p < .01$ compared to A431 tumors at both time points), respectively, resulting in a tumor to muscle ratio of 4.6 and 12.8. Administration of a 1 mg unlabeled panitumumab blocking dose significantly inhibited the uptake of ^{89}Zr-panitumumab in HCT116 tumors (5.0 ± 0.4% at

120 hours, $p < .01$ compared to nonblocked HCT116 tumors) to levels similar in EGFR-negative tumors. The uptake in T47D and MDA-MB435 tumors at 120 hours was 5.8 6 1.7% ID/g and 4.8 ± 1.9% ID/g, respectively ($p < .001$ compared to A431 and HCT116 tumors). The circulating levels of ^{89}Zr-panitumumab in the blood declined from 21.2 ± 0.9% ID/g at 24 hours to 12.3 ± 1.8% ID/g ($p < .001$) at 120 hours. Spleen uptake was 4.8 ± 0.2% ID/g and 4.4 ± 0.7% ID/g at 24 and 120 hours, respectively. Lung uptake was 9.9 ± 1.3% ID/g at 24 hours and declined to 6.5 ± 0.9% ID/g at 120 hours. Bone uptake was 3.0 ± 0.5% ID/g at 24 hours and 5.8 ± 1.6% ID/g at 120 hours. Liver accumulation of ^{89}Zr-panitumumab was limited to 8.8 ± 1.8% ID/g at 24 hours and remained constant at 120 hours. Kidney uptake was minimal. The uptake for each selected organ at 24 and 120 hours is demonstrated in Figure 3.

Imaging Studies

MicroPET/CT imaging studies demonstrated high uptake of ^{89}Zr-panitumumab in A431 tumors. The intensity of radio-tracer uptake was moderate in HCT116 tumors at 24 and 120 hours when compared to A431 tumors (Figure 4). The SUV_{max} for ^{89}Zr-Df-Bz-NCS-panitumumab for A431 and HCT116 tumors was 3.3 ± 0.3 and 2.7 ± 0.2 at 24hours ($p = .04$). At 120 hours, the SUV_{max} was 7.1 ± 0.9 and 4.0 ± 0.3 at 120 hours ($p = .005$) for the A431 and HCT116 tumors, respectively. Similar to the biodistribution study, the addition of excess cold unlabeled panitumumab significantly diminished uptake of ^{89}Zr-panitumumab in HCT116 tumors (SUV_{max} 1.84 ± 0.08 at 24 hours and 2.52 ± 0.07 at 120 hours; $p < .01$ at both time points). The uptake of T47D and MDA-MB435 tumors was minimal compared to background. The SUV_{max} of T47D was 1.01 ± 0.52 at 24 hours and 1.69 ± 0.70 at 120 hours. For the MDA-MB435 tumors, the SUV_{max} was 1.00 ± 0.39 at 24 hours and 1.08 ± 0.18 at 120 hours. The level of ^{89}Zr-panitumumab in the blood significantly decreased from 24 to 120 hours as evidenced by visualization of the blood pool in the heart and the inferior vena cava. Similarly, the uptake in liver from 24 to 120 hours was reduced. Figure 5 is a graphical representation of the SUV_{max} values for the evaluated tumors.

Immunohistochemistry

To confirm that EGFR expression levels in tumors correlated with EGFR expression in vitro, immunofluorescence staining was performed with an anti-EGFR antibody. Images were acquired under the same conditions and displayed on the same scale to ensure that the relative brightness observed in images reflected differences in EGFR expression level. The intensity EGFR staining (red) correlated to that observed with flow cytometry and was greatest in A431 tumors, moderate in HCT116 tumors, and negative in T47D and MDA-MB435 tumors. DAPI (blue) was used as the counterstain for the nucleus (Figure 6).

Discussion

In this study, a new PET agent was developed and characterized for the quantification of EGFR expression and for the monitoring of panitumumab uptake. In vitro cell association studies demonstrated a direct relationship between EGFR expression and ^{89}Zr-panitumumab uptake. Similarly, a linear association was seen between EGFR expression and intratumoral uptake of ^{89}Zr-panitumumab by microPET/CT imaging as shown in Figure 7. At 24 hours,

the highest level of radiotracer accumulation was observed in the A431 vulvar epidermoid carcinoma tumors, which also expressed the highest level of EGFR. Moderate uptake was seen in HCT116 colorectal tumors that express moderate levels of EGFR. Minimal to no uptake was observed in the T47D and MDA-MB435 EGFR-negative breast tumors. A significant amount of circulating ^{89}Zr-panitumumab was seen at 24 hours, as evidenced by the elevated intensity in the heart and abdominal aorta on imaging and confirmed in the biodistribution studies. From 24 to 120 hours, the circulating level of ^{89}Zr-panitumumab declined, whereas the tracer continued to accumulate in EGFR-positive tumors as demonstrated by the rise in SUV_{max} on microPET/CT imaging and tumor uptake in the biodistribution studies. The inhibition of ^{89}Zr-panitumumab uptake in the HCT116 EGFR-positive tumors with preadministration of excess unlabeled panitumumab demonstrated the specificity of the radiotracer.

Several approaches have been evaluated for the imaging of EGFR. Although small molecule inhibitors radiolabeled with ^{11}C, ^{123}I, ^{125}I, and ^{18}F have demonstrated promise in vitro,[31–34] the majority of these compounds resulted in low-quality images with low tumor to background ratios.[35] Anti-EGFR monoclonal antibodies radiolabeled with ^{64}Cu, ^{86}Y, ^{88}Y, ^{89}Zr, ^{111}In, and ^{125}I have demonstrated improved specificity over the radiolabeled small molecule inhibitors for tumors overexpressing EGFR.[11–20] However, the limitation to many of these radiolabeled antibodies, particularly observed in images obtained with ^{111}In and ^{64}Cu, was the high liver uptake, ranging from 15 to 47% ID/g.[11,13,15] Transchelation of the radionuclide to liver proteins has been shown to play a significant role in liver uptake.[15] Elevated liver uptake limits the amount of administered activity and often results in a low tumor to liver ratio.[13–15,36]

In the current study, the liver uptake was low when compared to the studies performed with ^{64}Cu- and ^{111}In-radiolabeled anti-EGFR antibodies.[11,13,15] Multiple factors may explain the lower level of liver uptake. Given that ^{89}Zr is relatively biologically inert in comparison with iodine or copper, which have known cellular transporters, ^{89}Zr may be less likely to react with the liver proteins and transchelate. Also, the high stability of the ^{89}Zr-desferrioxamine chelate complex, as demonstrated in the serum stability studies, may result in minimal transchelation. The liver uptake values observed in this study are in close agreement with Nayak and colleagues, who recently reported similar liver uptake values with yttrium 86– radiolabeled panitumumab.[20]

An elevated uptake of ^{89}Zr in bone was observed with several ^{89}Zr-radiolabeled antibodies.[37,38] At 120 hours postinjection, biodistribution studies demonstrated that the bone uptake was 5.7 ± 3.0% ID/g, which is in agreement with previous studies using desferrioxamine as a chelator. This uptake was well visualized in the axillary and mandibular joints of the mice. This elevated bone uptake may be a limitation for determining pharmacokinetic distribution of the antibody to the bone. The process of transchelation of ^{89}Zr to the bone has not been elucidated. Intratumoral metabolism has been suggested, but our stability studies, along with other previous studies with ^{89}Zr-radiolabeled antibodies, suggest that this is limited. Although beyond the scope of the current study, future studies are under way to evaluate novel chelators with improved stability for zirconium.

Previous studies have evaluated the use of radiolabeled anti-EGFR antibodies for in vivo determination of EGFR expression level, with mixed results. In the current study, ^{89}Zr-panitumumab uptake highly correlated with the level of EGFR expression in tumors, as shown in Figure 7. An association between ^{111}In-radiolabeled cetuximab uptake and EGFR expression level has been reported.[11] Similarly, Cai and colleagues demonstrated a correlation between ^{64}Cu-radiolabeled cetuximab uptake and EGFR expression level in mouse xenograft models of glioblastoma, prostate carcinoma, colorectal carcinoma, and breast cancer.[14] In contrast, the same group was not able to see a correlation between ^{64}Cu-radiolabeled panitumumab uptake and EGFR expression level in head and neck squamous cell carcinoma mouse xenograft models.[18] Furthermore, other discrepancies in ^{89}Zr-radiolabeled cetuximab uptake and EGFR expression have been reported.[19] Multiple factors, including partial volume effects, differences in injected antibody concentration, and different imaging time points, may explain these contrasting results. Also, the enhanced permeability and retention factor has been suggested to play a major role in nonspecific antibody uptake. This effect is greater as tumor size increases and leads to increased nonspecific extravasation of macromolecules. The effect is greatest at early time points and steadily decreases thereafter.[39] In our study, the tumor size was limited to 150 to 200 mm^3 to minimize the enhanced permeability and retention factor and partial volume effects. Moreover, the use of ^{89}Zr allowed for imaging at later time points in which the enhanced permeability and retention effect was minimized.

^{89}Zr-panitumumab is unable to detect EGFR mutations and mutations in downstream signaling proteins such as Kras and PTEN, which limit the benefit of anti-EGFR therapy.[40–42] In malignancies such as colorectal cancer and pancreatic cancer, the presence of these mutations can be significant. Therefore, ^{89}Zr-panitumumab may be used to guide treatment selection once wild-type EGFR, Kras, and PTEN status have been determined and may be used to monitor the response to anti-EGFR treatments. In malignancies such as head and neck and esophageal cancer, Kras and PTEN mutations are rare. Therefore, ^{89}Zr-panitumumab may be used to select patients for anti-EGFR treatment in these malignancies.

The strength of using ^{89}Zr for immunoPET is the extended half-life of 78.4 hours.[27] Serial imaging can be performed to follow the pharmacokinetics of antibodies, which take approximately 96 hours to equilibrate within the body. In addition, once internalized, ^{89}Zr is trapped intracellularly,[27] providing a more accurate measurement of the uptake of internalizing antibodies in comparison with radionuclides such as ^{124}I and ^{64}Cu, which can be exported extracellularly. A concern with patient administration of ^{89}Zr is the mean radiation dose to the patient and the risk of public exposure with the 909 keV gamma decay. Although dosimetry experiments were beyond the scope of this study, clinical trials in Europe have demonstrated the feasibility and safety of ^{89}Zr-radiolabeled antibodies at administered activities of 37 to 74 MBq.[27,43,44]

Conclusion

In vivo imaging of the EGFR was successfully performed with ^{89}Zr-panitumumab. This probe can be used to evaluate the relative levels of EGFR expression within a tumor and be used to scout the biodistribution of panitumumab to individualize patient dosing.

Furthermore, the two-step facile preparation method expedites the translation of ^{89}Zr-panitumumab for clinical evaluation.

Acknowledgments

We would like to thank Bill Margenau for reliable cyclotron operation.

References

1. Lurje G, Lenz HJ. EGFR signaling and drug discovery. Oncology. 2009; 77:400–410. [PubMed: 20130423]
2. Mendelsohn J, Baselga J. Epidermal growth factor receptor targeting in cancer. Semin Oncol. 2006; 33:369–485. [PubMed: 16890793]
3. Yarden Y, Sliwkowski MX. Untangling the ErbB signalling network. Nat Rev. 2001; 2:127–137.
4. Kotsakis A, Georgoulias V. Targeting epidermal growth factor receptor in the treatment of non-small-cell lung cancer. Expert Opin Pharmacother. 2010; 11:2363–2389. [PubMed: 20586711]
5. Grothey A. EGFR antibodies in colorectal cancer: where do they belong? J Clin Oncol. 2010; 28:4668–4670. [PubMed: 20921457]
6. Panitomumab. [accessed July 20, 2012] Available at: http://Clinicaltrials.gov.
7. Yang BB, Lum P, Chen A, et al. Pharmacokinetic and pharmacodynamic perspectives on the clinical drug development of panitumumab. Clin Pharmacokinet. 2010; 49:729–740. [PubMed: 20923247]
8. Hecht JR, Mitchell E, Neubauer MA, et al. Lack of correlation between epidermal growth factor receptor status and response to panitumumab monotherapy in metastatic colorectal cancer. Clin Cancer Res. 2010; 16:2205–2213. [PubMed: 20332321]
9. Tol J, Punt CJ. Monoclonal antibodies in the treatment of metastatic colorectal cancer: a review. Clin Ther. 2010; 32:437–453. [PubMed: 20399983]
10. McCabe KE, Wu AM. Positive progress in immunoPET—not just a coincidence. Cancer Biother Radiopharm. 2010; 25:253–261. [PubMed: 20578830]
11. Goldenberg A, Masui H, Divgi C, et al. Imaging of human tumor xenografts with an indium-111-labeled anti-epidermal growth factor receptor monoclonal antibody. J Natl Cancer Inst. 1989; 81:1616–1625. [PubMed: 2795690]
12. Perk LR, Visser GW, Vosjan MJ, et al. (89)Zr as a PET surrogate radioisotope for scouting biodistribution of the therapeutic radiometals (90)Y and (177)Lu in tumor-bearing nude mice after coupling to the internalizing antibody cetuximab. J Nucl Med. 2005; 46:1898–1906. [PubMed: 16269605]
13. Wen X, Wu QP, Ke S, et al. Conjugation with (111)In-DTPA-poly(ethylene glycol) improves imaging of anti-EGF receptor antibody C225. J Nucl Med. 2001; 42:1530–1537. [PubMed: 11585869]
14. Cai W, Chen K, He L, et al. Quantitative PET of EGFR expression in xenograft-bearing mice using 64Cu-labeled cetuximab, a chimeric anti-EGFR monoclonal antibody. Eur J Nucl Med Mol Imaging. 2007; 34:850–858. [PubMed: 17262214]
15. Ping, Li W.; Meyer, LA.; Capretto, DA., et al. Receptor-binding, biodistribution, and metabolism studies of 64Cu-DOTA-cetuximab, a PET-imaging agent for epidermal growth-factor receptor-positive tumors. Cancer Biother Radiopharm. 2008; 23:158–171. [PubMed: 18454685]
16. Nayak TK, Regino CA, Wong KJ, et al. PET imaging of HER1-expressing xenografts in mice with 86Y-CHX-A”-DTPA-cetuximab. Eur J Nucl Med Mol Imaging. 2010; 37:1368–1376. [PubMed: 20155263]
17. Niu G, Sun X, Cao Q, et al. Cetuximab-based immunotherapy and radioimmunotherapy of head and neck squamous cell carcinoma. Clin Cancer Res. 2010; 16:2095–2105. [PubMed: 20215534]
18. Niu G, Li Z, Xie J, et al. PET of EGFR antibody distribution in head and neck squamous cell carcinoma models. J Nucl Med. 2009; 50:1116–1123. [PubMed: 19525473]

19. Aerts HJ, Dubois L, Perk L, et al. Disparity between in vivo EGFR expression and 89Zr-labeled cetuximab uptake assessed with PET. J Nucl Med. 2009; 50:123–131. [PubMed: 19091906]
20. Nayak TK, Garmestani K, Milenic DE, et al. HER1-targeted Y-panitumumab possesses superior targeting characteristics than Y-cetuximab for PET imaging of human malignant mesothelioma tumors xenografts. PLoS One. 2011; 6:e18198. [PubMed: 21464917]
21. Nayak TK, Garmestani K, Baidoo KE, et al. Preparation, biological evaluation, and pharmacokinetics of the human anti-HER1 monoclonal antibody panitumumab labeled with 86Y for quantitative PET of carcinoma. J Nucl Med. 2010; 51:942–950. [PubMed: 20484421]
22. van Dongen GA, Visser GW, Lub-de Hooge MN, et al. Immuno-PET: a navigator in monoclonal antibody development and applications. Oncologist. 2007; 12:1379–1389. [PubMed: 18165614]
23. Perk LR, Vosjan MJ, Visser GW, et al. p-Isothiocyanatobenzyl-desferrioxamine: a new bifunctional chelate for facile radiolabeling of monoclonal antibodies with zirconium-89 for immuno-PET imaging. Eur J Nucl Med Mol Imaging. 2010; 37:250–259. [PubMed: 19763566]
24. van Dongen GA, Vosjan MJ. Immuno-positron emission tomography: shedding light on clinical antibody therapy. Cancer Biother Radiopharm. 2010; 25:375–385. [PubMed: 20707716]
25. Dijkers EC, Oude Munnink TH, Kosterink JG, et al. Biodistribution of 89Zr-trastuzumab and PET imaging of HER2-positive lesions in patients with metastatic breast cancer. Clin Pharmacol Ther. 2010; 87:586–592. [PubMed: 20357763]
26. Oude Munnink TH, Korte MA, Nagengast WB, et al. (89)Zr-trastuzumab PET visualises HER2 downregulation by the HSP90 inhibitor NVP-AUY922 in a human tumour xenograft. Eur J Cancer. 2010; 46:678–684. [PubMed: 20036116]
27. Borjesson PK, Jauw YW, de Bree R, et al. Radiation dosimetry of 89Zr-labeled chimeric monoclonal antibody U36 as used for immuno-PET in head and neck cancer patients. J Nucl Med. 2009; 50:1828–1836. [PubMed: 19837762]
28. Perk LR, Stigter-van Walsum M, Visser GW, et al. Quantitative PET imaging of Met-expressing human cancer xenografts with 89Zr-labelled monoclonal antibody DN30. Eur J Nucl Med Mol Imaging. 2008; 35:1857–1867. [PubMed: 18491091]
29. Verel I, Visser GW, Boellaard R, et al. 89Zr immuno-PET: comprehensive procedures for the production of 89Zr-labeled monoclonal antibodies. J Nucl Med. 2003; 44:1271–1281. [PubMed: 12902418]
30. Holland JP, Sheh Y, Lewis JS. Standardized methods for the production of high specific-activity zirconium-89. Nucl Med Biol. 2009; 36:729–739. [PubMed: 19720285]
31. Mishani E, Abourbeh G. Cancer molecular imaging: radionuclide-based biomarkers of the epidermal growth factor receptor (EGFR). Curr Top Med Chem. 2007; 7:1755–1772. [PubMed: 17979785]
32. Mishani E, Abourbeh G, Eiblmaier M, Anderson CJ. Imaging of EGFR and EGFR tyrosine kinase overexpression in tumors by nuclear medicine modalities. Curr Pharm Des. 2008; 14:2983–2998. [PubMed: 18991714]
33. Memon AA, Jakobsen S, Dagnaes-Hansen F, et al. Positron emission tomography (PET) imaging with [11C]-labeled erlotinib: a micro-PET study on mice with lung tumor xenografts. Cancer Res. 2009; 69:873–878. [PubMed: 19155297]
34. Liu N, Li M, Li X, et al. PET-based biodistribution and radiation dosimetry of epidermal growth factor receptor-selective tracer 11C-PD153035 in humans. J Nucl Med. 2009; 50:303–308. [PubMed: 19164239]
35. Mishani E, Hagooly A. Strategies for molecular imaging of epidermal growth factor receptor tyrosine kinase in cancer. J Nucl Med. 2009; 50:1199–1202. [PubMed: 19617320]
36. Lovdal T, Andersen E, Brech A, Berg T. Fc receptor mediated endocytosis of small soluble immunoglobulin G immune complexes in Kupffer and endothelial cells from rat liver. J Cell Sci. 2000; 113(Pt 18):3255–3266. [PubMed: 10954423]
37. Holland JP, Caldas-Lopes E, Divilov V, et al. Measuring the pharmacodynamic effects of a novel Hsp90 inhibitor on HER2/neu expression in mice using Zr-DFO-trastuzumab. PLoS One. 2010; 5:e8859. [PubMed: 20111600]
38. Borjesson PK, Jauw YW, Boellaard R, et al. Performance of immuno-positron emission tomography with zirconium-89-labeled chimeric monoclonal antibody U36 in the detection of

lymph node metastases in head and neck cancer patients. Clin Cancer Res. 2006; 12:2133–2140. [PubMed: 16609026]

39. de Bree R, Kuik DJ, Quak JJ, et al. The impact of tumour volume and other characteristics on uptake of radiolabelled monoclonal antibodies in tumour tissue of head and neck cancer patients. Eur J Nucl Med. 1998; 25:1562–1565. [PubMed: 9799354]
40. Sartore-Bianchi A, Bencardino K, Cassingena A, et al. Therapeutic implications of resistance to molecular therapies in metastatic colorectal cancer. Cancer Treat Rev. 2010; 36(Suppl 3):S1–S5. [PubMed: 21129603]
41. De Roock W, Claes B, Bernasconi D, et al. Effects of KRAS, BRAF, NRAS, and PIK3CA mutations on the efficacy of cetuximab plus chemotherapy in chemotherapy-refractory metastatic colorectal cancer: a retrospective consortium analysis. Lancet Oncol. 2010; 11:753–762. [PubMed: 20619739]
42. Bardelli A, Siena S. Molecular mechanisms of resistance to cetuximab and panitumumab in colorectal cancer. J Clin Oncol. 2010; 28:1254–1261. [PubMed: 20100961]
43. Hoeben BA, Kaanders JH, Franssen GM, et al. PET of hypoxia with 89Zr-labeled cG250-F(ab')2 in head and neck tumors. J Nucl Med. 2010; 51:1076–1083. [PubMed: 20554724]
44. Dijkers EC, Oude Munnink TH, Kosterink JG, et al. Biodistribution of 89Zr-trastuzumab and PET imaging of HER2-positive lesions in patients with metastatic breast cancer. Clin Pharmacol Ther. 2010; 87:586–592. [PubMed: 20357763]

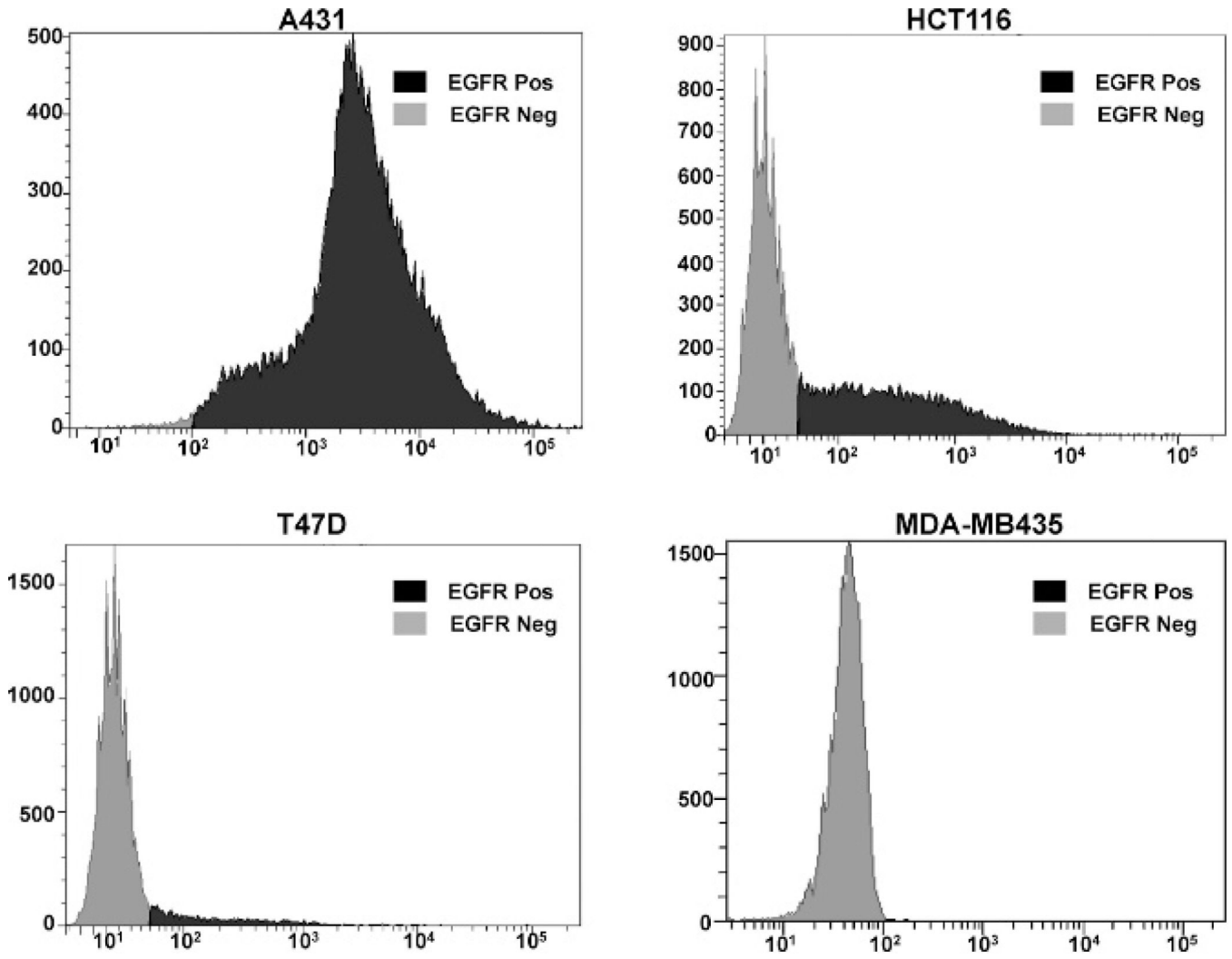

Figure 1.

Flow cytometric analysis of epidermal growth factor receptor (EGFR) expression. The A431 epidermoid carcinoma, HCT116 colorectal cancer, T47D breast cancer, and MDA-MB435 breast cancer cell lines were evaluated for EGFR expression. Panitumumab was used as the primary antibody, and FITC-conjugated goat antihuman IgG was used as the secondary antibody. Data are shown as cell number on the ordinate access and EGFR intensity on the abscissa.

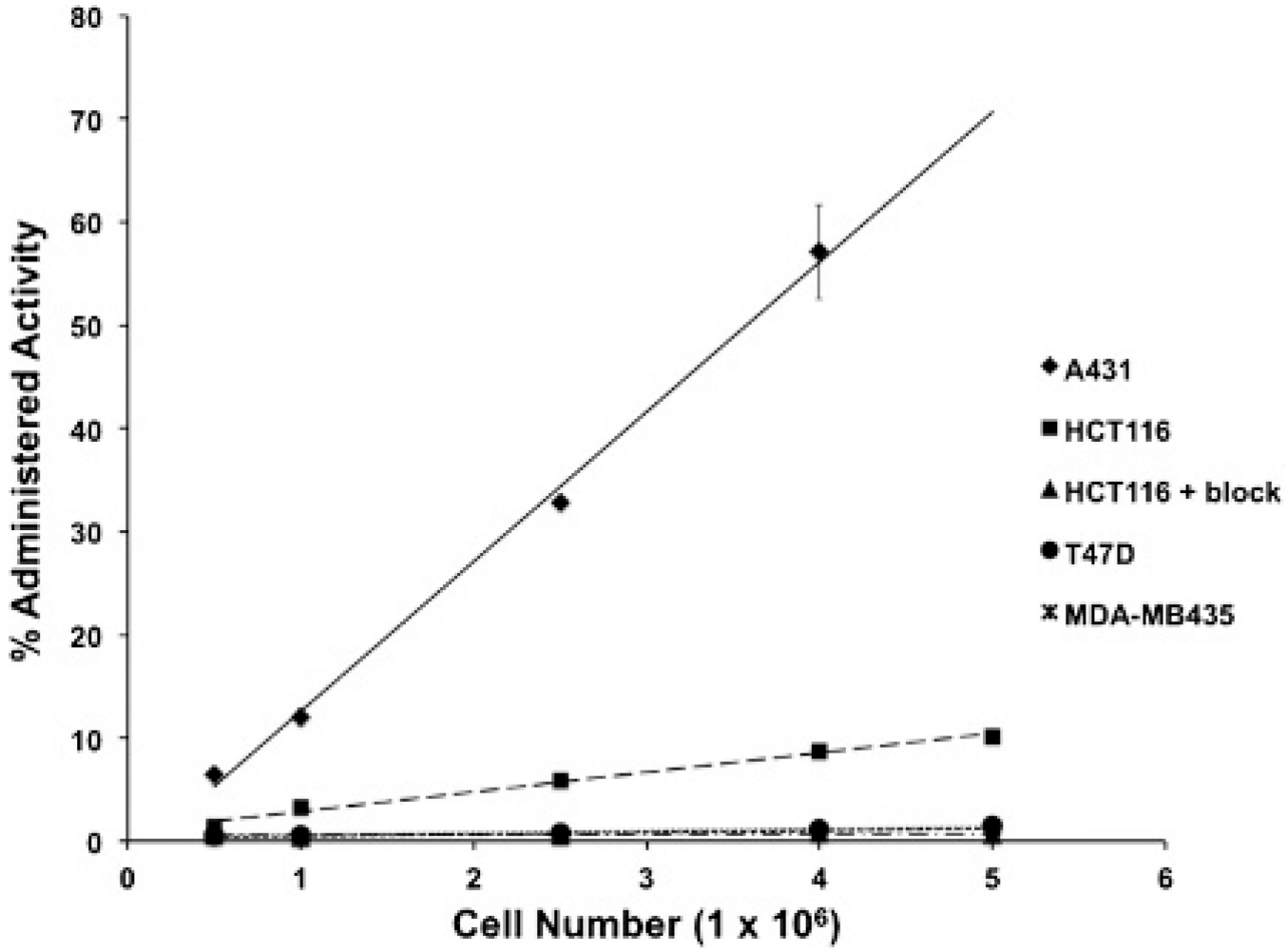

Figure 2.

Cell uptake studies with ^{89}Zr-panitumumab. Cell uptake curves of cell number versus percentage of administered activity in A431, HCT116, T47D, and MDA-MB435 cells (n = 3).

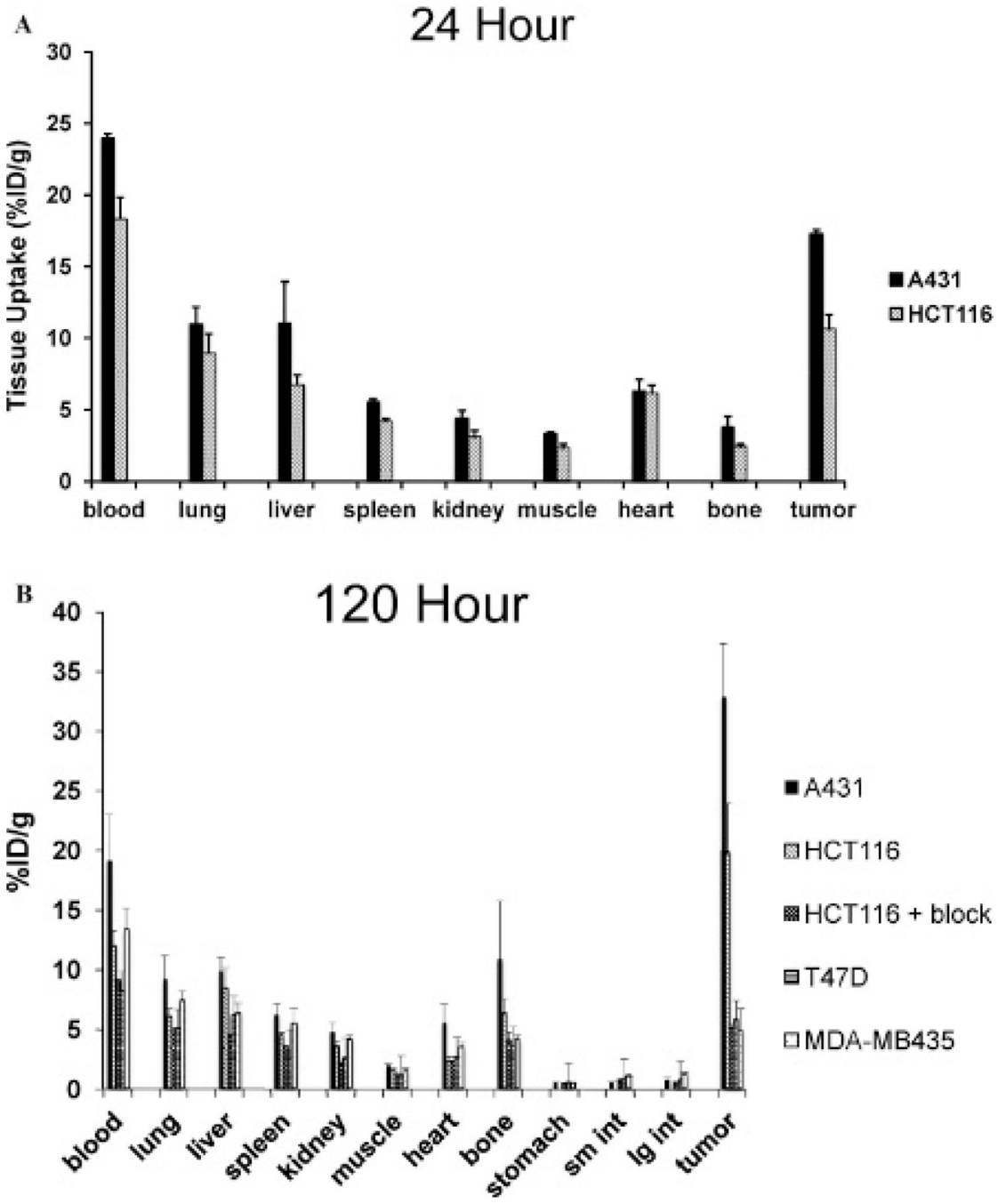

Figure 3.

Biodistribution of ^{89}Zr-panitumumab in A431, HCT116, T47D, and MDA-MB435 xenograft models at 24 (A) and 120 (B) hours postinjection. A 1 mg blocking dose of panitumumab was administered 120 minutes prior to administration of ^{89}Zr-panitumumab. Data are expressed as percent injected dose per gram ± standard deviation, $n = 5$ for each time point.

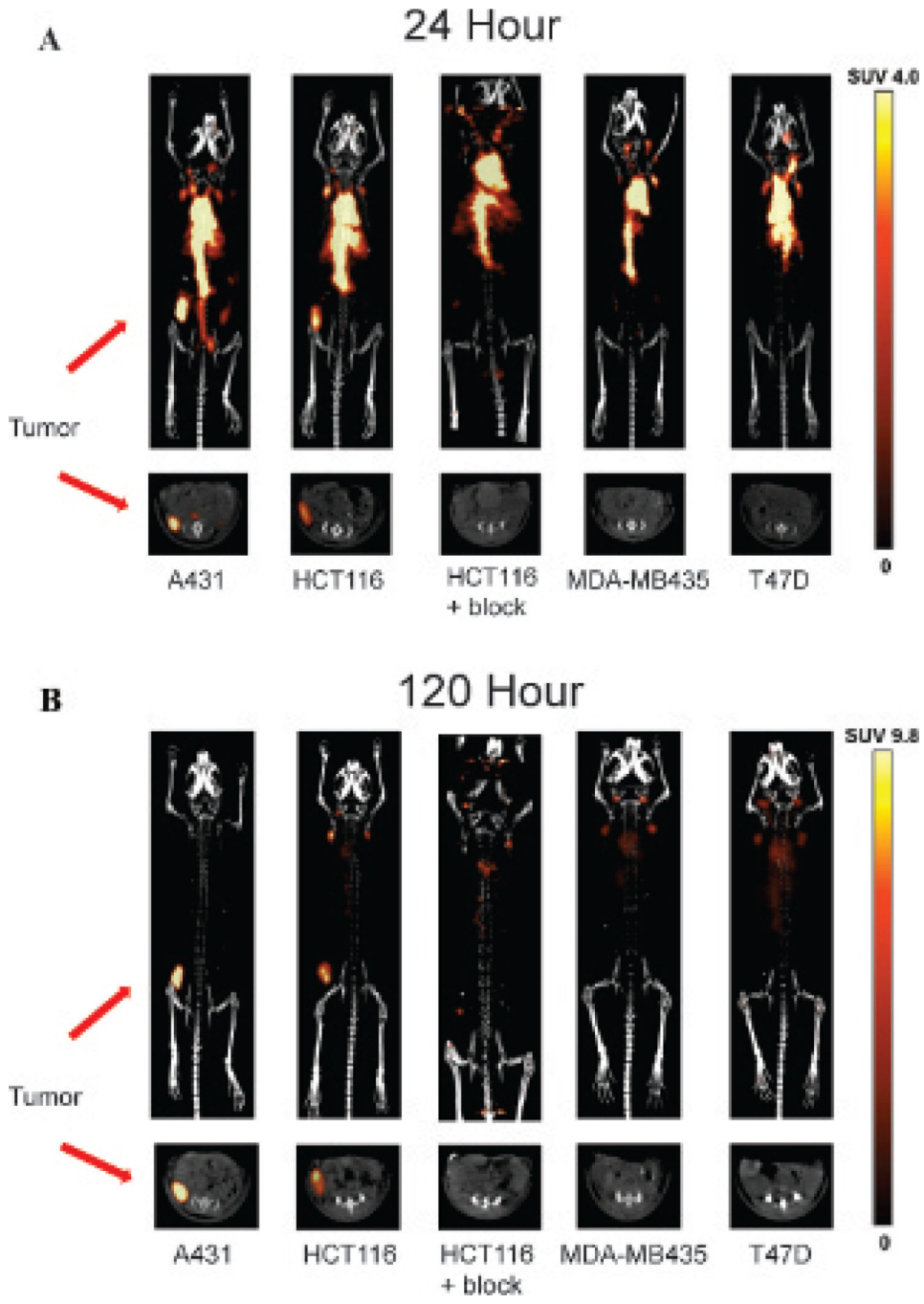

Figure 4.

Representative microPET/CT images obtained at 24 (A) and 120 (B) hours. Tumors were located in the right flank of each mouse. Maximum intensity projected reconstructions are demonstrated in the *upper panels*, and the axial slice at the center of the tumor is shown in the *bottom panel*. The scale, expressed as standardized uptake value (SUV), is demonstrated at the far right. A 1 mg blocking dose of panitumumab was administered 120 minutes prior to injection of ^{89}Zr-panitumumab.

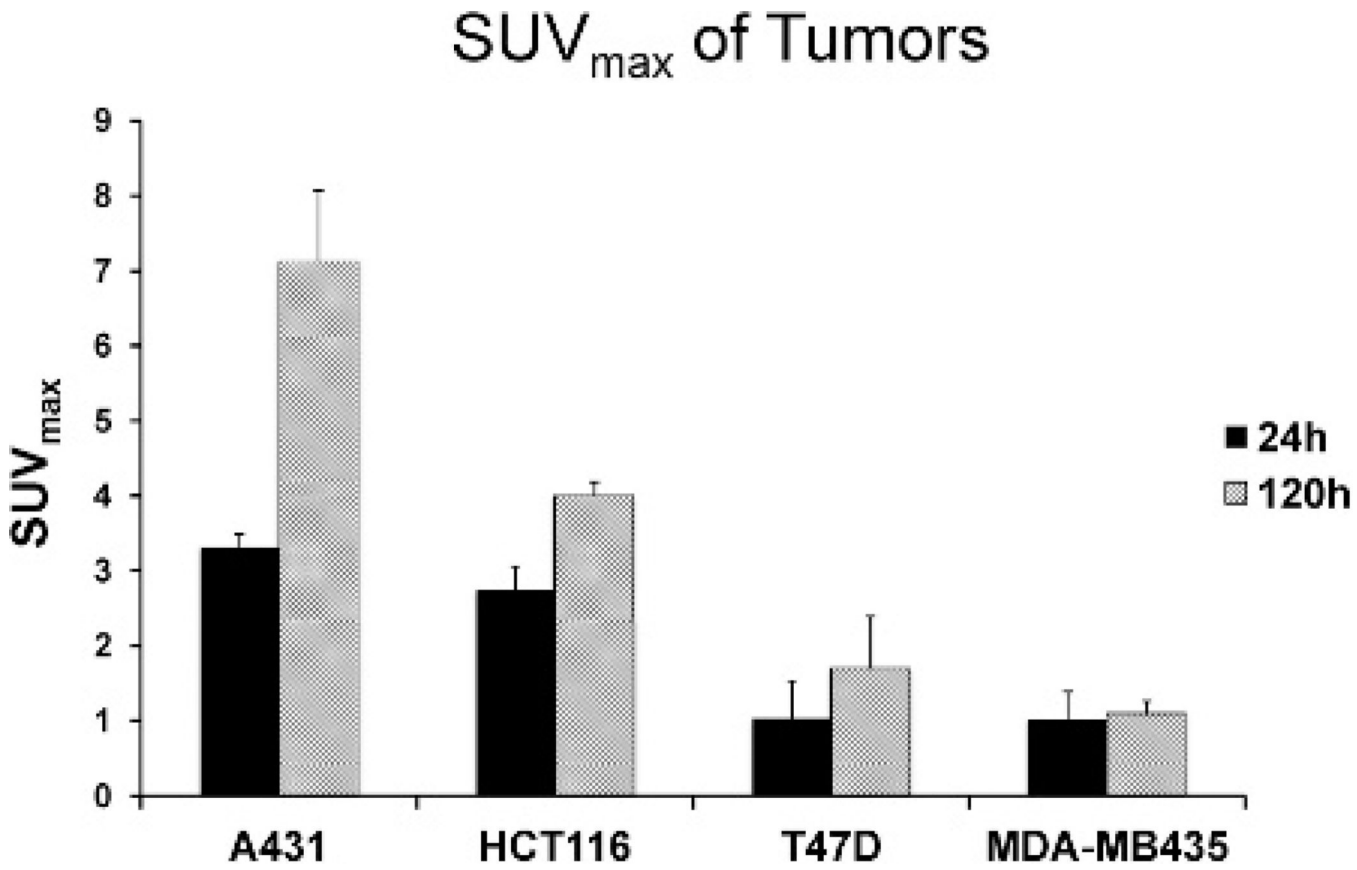

Figure 5.

A graphical analysis of ^{89}Zr-panitumumab uptake in xenograft tumor models expressed as standardized uptake value (SUV) ± standard deviation for each tumor type.

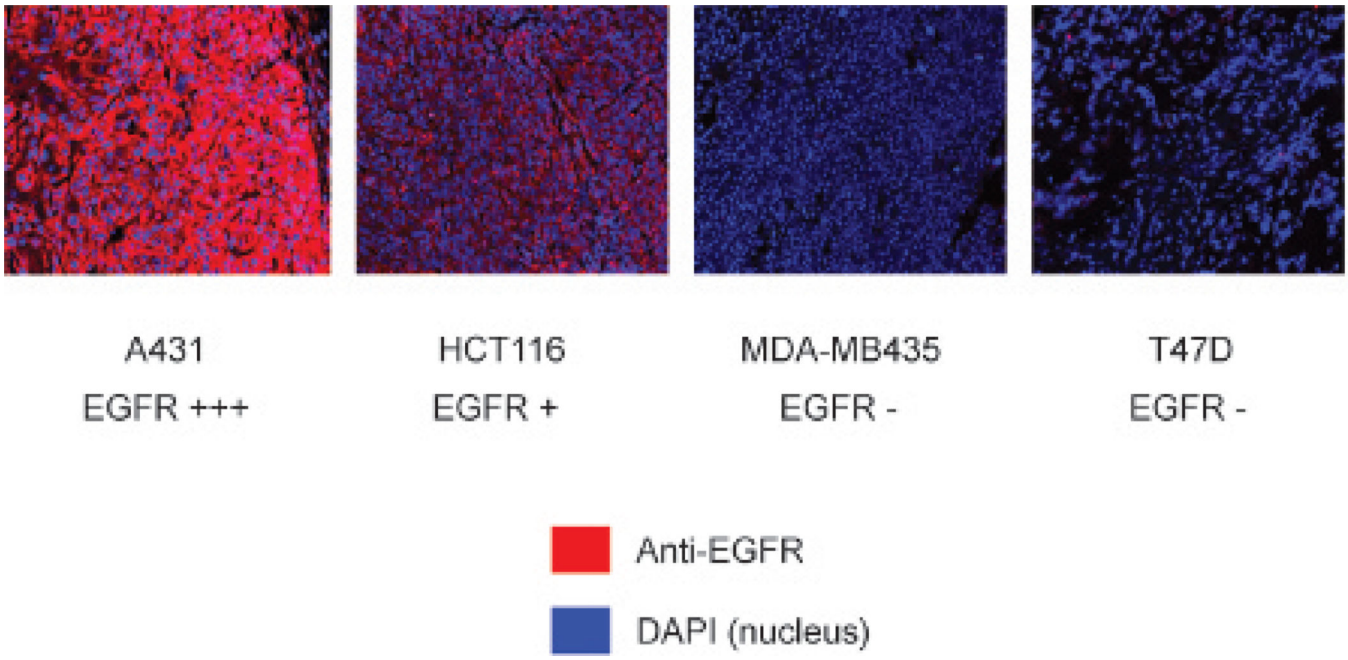

Figure 6.

Immunofluorescent staining to evaluate the relative levels of epidermal growth factor receptor (EGFR) expression for each tumor type. EGFR staining is demonstrated in red, with a counterstain for the nucleus in blue.

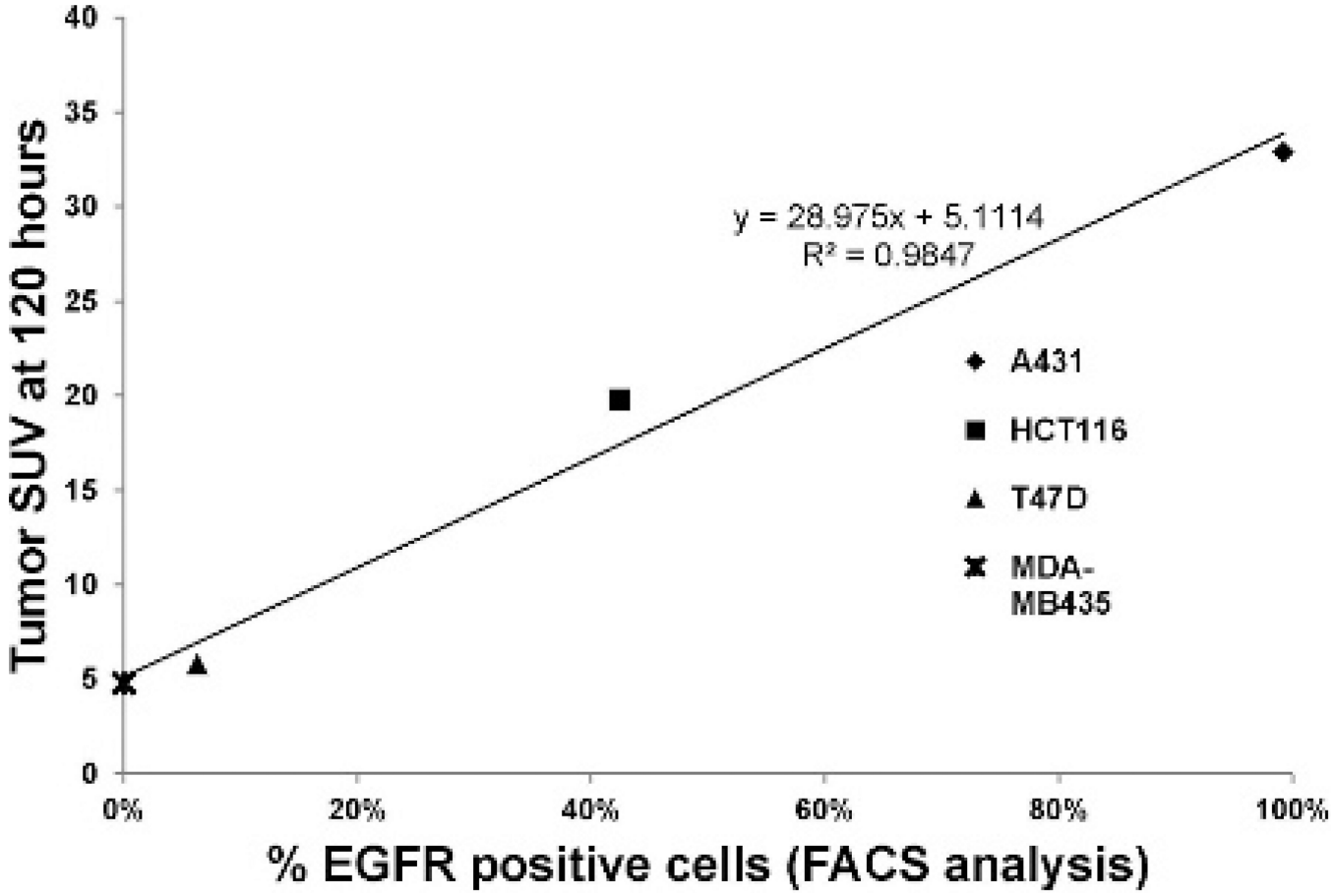

Figure 7.

Linear correlation between cell line epidermal growth factor receptor (EGFR) expression (as determined by FACS, as shown in Figure 1) and standardized uptake value (SUV) of tumor xenografts with the same cell lines (from Figure 4B).